THEORETICAL EVIDENCE FOR STATIONARY SIZE DISTRIBUTION OF OXIDE NANOPARTICLES IN DISPERSION STRENGTHENED STEEL UNDER CASCADE PRODUCING IRRADIATION

Alexander Borisenko

National Science Center "Kharkov Institute of Physics and Technology", Kharkiv, Ukraine
E-mail: borisenko@kipt.kharkov.ua

A model developed in this paper describes the transport of nonequilibrium (produced by irradiation) point defects across a coherent interface in a heterophase medium. In the framework of this model we derive a kinetic equation for the distribution function of spherical nanoparticles of the second phase in a solid solution, which accounts for the flow and diffusion of nanoparticles in the dimension space as well as their dissolution in atomic collision cascades. We obtain an analytical form and study the stationary solution of this equation. The result obtained fits well to experimental data [A. Certain et al. Journal of Nuclear Materials. (2013) 434, 311] on distribution of Y-Ti-O nanoparticles in the oxide dispersion strengthened ferritic steel 14YWT, irradiated with nickel ions up to 100 dpa at different temperatures. We conclude that in this case irradiation affects the distribution of fine oxide nanoparticles by creating nonequilibrium point defects rather than by cascade mixing.

INTRODUCTION

Phase transformations in solids under irradiation have been subject to intensive studies for a long time (see e.g. [1, 2] for reference). Besides, these studies are actual for R&D of novel structural materials for nuclear applications. During previous decades a lot of effort has been applied to investigation of the so-called Oxide Dispersion Strengthened (ODS) steels. These steels are considered prospective because they preserve satisfactory mechanical characteristics at temperatures up to 700 °C and radiation damage doses up to 150 displacements per atom (dpa) due to the presence of a dence (concentration $\sim 10^{23}\,\mathrm{m}^{-3}$) dispersion of nanosized particles based on Y-Ti-O composition in the matrix. Nowadays active studies of irradiation impact on the stability of this dispersion are underway.

If irradiation is absent, the second phase dispersion in a supersaturated solid matrix is usually unstable: the cube of the mean particle size grows linearly with time due to the effect of Ostwald ripening [3]. The effect of cascade-producing irradiation is as follows: atomic collision cascades, produced by high-energy neutrons or ions, give rise to mixing of solute and matrix atoms and trap the temporal evolution of nanoparticles to the cycle: nucleation – diffusion growth – cascade dissolution.

The model of homogeneous semicoherent intephase boundary [4] has been previously proposed to explain the effect of nonequilibrium point defects (PD) on the kinetics of phase transformations in solids under cascadeless (electron) irradiation. The recent papers [5–7] study the contribution of heterophase fluctuations to solubility and nucleation rate of second phases in solid solutions at non-radiation conditions. In this paper we develop the above models and apply them to study the stability of the second phase dispersion with coherent interface in an alloy under cascade-producing (ion or neutron) irradiation.

1. A MODEL OF THE SOLUTE ATOM TRANSPORT IN A HETEROPHASE STRUCTURE WITH A COHERENT INTERFACE

Consider an interphase boundary (Gibbs interface) between a stoichiometric particle (*p*), consisting of atoms of several types, labeled $j \in p$, and a solution of these atoms in a solid matrix (*m*). Let the interface between the particle and the matrix be coherent, i.e. the atomic planes be continuous across it. Since the bulk physical properties of such heterophase structure are discontinuous across the interface, the PD number density (concentration) profiles are expected to be discontinuous as well. The PD can penetrate across the interface via a thermal activation mechanism. Therefore, the PD transfer across the interface can be considered as a reversible surface chemical reaction.

1.1. TRANSFER OF POINT DEFECTS ACROSS THE INTERFACE

An interstitial atom of the type *j*, located at one side of the interface, can transfer to the other side of the interface and vice versa. This process can be represented in the form of a reversible chemical reaction:

$$i_j^p \leftrightarrow i_j^m, \tag{1}$$

where i_j^φ denotes an interstitial of the type *j* in the particle $(\varphi = p)$ or in the matrix $(\varphi = m)$.

In this way, the rate of transitions, represented by Eq. (1), in each direction, is proportional to the concentration $c_{i_j}^\varphi$ of the interstitials i_j^φ in the corresponding phase and the normal component of the flux of *j*-type atoms across the interface via the interstitial mechanism is

as follows (hereinafter the normal unit vector is supposed to be directed from the particle into the matrix):

$$J_{i_j} = \omega_0 \beta_{i_j}^p c_{i_j}^p - \omega_0 \beta_{i_j}^m c_{i_j}^m, \tag{2}$$

where ω_0 is a mean unit atomic volume. The kinetic coefficients in Eq. (2) are assumed to depend on temperature according to the Arrhenius's law: $\beta_{i_j}^\varphi \propto \exp\left(-G_{i_j}^\varphi / k_B T\right)$, where $G_{i_j}^\varphi$ is an activation energy of transfer across the interface of the j-type interstitial in the corresponding phase; k_B is the Boltzmann's constant; T is temperature.

An atom of the type j, located at a regular lattice site at one side of the interface, can transfer to a neighboring vacant site at the other side of the interface and vice versa. This process can be represented in the form of a reversible chemical reaction:

$$l_j^m + v_j^p \leftrightarrow l_j^p + v^m, \tag{3}$$

where l_j^m is an atom of the type j at the matrix lattice site; v_j^p is a vacant lattice site in the j-th sublattice of the particle; l_j^p is an atom in the j-th sublattice of the particle; v^m is a vacant lattice site in the matrix.

Therefore, the rate of transitions, represented by Eq. (3), in each direction, should be bilinear in the concentrations of the corresponding species and the normal component of the flux of j-type atoms across the interface via the vacancy mechanism is as follows:

$$J_{v_j} = \omega_0 \delta_{v_j}^m c_v^m c_{l_j}^p - \omega_0 \delta_{v_j}^p c_{v_j}^p c_{l_j}^m. \tag{4}$$

Here $c_{v_j}^p$ is a concentration of vacancies in the j-th sublattice of the particle; $c_{l_j}^m$ is a concentration of the atoms j at lattice sites of the matrix; c_v^m is a concentration of vacancies in the matrix, and $c_{l_j}^p$ is a concentration of the atoms j at lattice sites of the particle.

Similarly to Eq. (2), the kinetic coefficients $\delta_{v_j}^\varphi$ in Eq. (4) are assumed to depend on temperature according to the Arrhenius's law, but with a different activation energy $G_{v_j}^\varphi$.

An interstitial atom located at one side of the interface can recombine with a vacancy located at the other side:

$$i_j^p + v^m \rightarrow l_j^m; \quad i_j^m + v_j^p \rightarrow l_j^p. \tag{5}$$
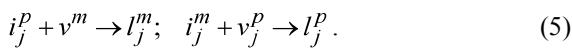
These are irreversible reactions because an energy threshold for production of the Frenkel pairs is usually large. The normal component of the flux of j-type atoms across the interface via the recombination mechanism (5) is as follows:

$$J_{R_j} = \omega_0 \alpha_{R_j}^p c_{i_j}^p c_v^m - \omega_0 \alpha_{R_j}^m c_{i_j}^m c_{v_j}^p, \tag{6}$$

where $\alpha_{R_j}^\varphi$ is a phenomenological recombination kinetic coefficient in the corresponding phase.

Therefore, the partial flux of j-type atoms across the interface is a sum of the contributions, given by Eqs. (2), (4), and (6):

$$J_j = J_{i_j} + J_{v_j} + J_{R_j}. \tag{7}$$

A total concentration of j-type atoms in the corresponding phase is a sum of the concentrations of the atoms in both the interstitial and regular positions: $c_j^\varphi = c_{i_j}^\varphi + c_{l_j}^\varphi$. One can consider the following relations between the concentrations of solute atoms in different lattice positions:

$$c_{i_j}^\varphi = x_j^\varphi c_j^\varphi; \quad c_{l_j}^\varphi = \left(1 - x_j^\varphi\right) c_j^\varphi, \tag{8}$$

where x_j^φ is a dimensionless constant, taking its value from the range $0 \le x_j^\varphi \le 1$. The lower and upper limiting values correspond to the cases when the solute atoms reside only in the regular and interstitial lattice positions, respectively. The value of x_j^φ depends on both interatomic potential and irradiation conditions.

Now, taking into account Eqs. (2), (4), (6), and (8), one can represent Eq. (7) as follows:

$$J_j = \omega_0 c_j^p \left[\beta_{i_j}^p x_j^p + \left(\delta_{v_j}^m \left(1 - x_j^p\right) + \alpha_{R_j}^p x_j^p \right) c_v^m \right] - \omega_0 c_j^m \left[\beta_{i_j}^m x_j^m + \left(\delta_{v_j}^p \left(1 - x_j^m\right) + \alpha_{R_j}^m x_j^m \right) c_{v_j}^p \right]. \tag{9}$$

The total atomic flux across the interface is

$$J = \sum_{j=1}^n J_j. \tag{10}$$

As a next approximation, we require that a chemical composition (stoichiometry) of the particle is conserved:

$$c_j^p = const_j, \quad j \in p. \tag{11}$$

Then the partial flux of atoms j across the interface (9) is related to the total atomic flux (10) as follows:

$$J_j = J c_j^p \omega_0. \tag{12}$$

Therefore, employing Eq. (9), one can represent the total atomic flux across the interface as follows:

$$J = \beta_{i_j}^p x_j^p + \left(\delta_{v_j}^m \left(1 - x_j^p\right) + \alpha_{R_j}^p x_j^p \right) c_v^m - \left[\beta_{i_j}^m x_j^m + \left(\delta_{v_j}^p \left(1 - x_j^m\right) + \alpha_{R_j}^m x_j^m \right) c_{v_j}^p \right] c_j^m / c_j^p. \tag{13}$$

The state of kinetic equilibrium at the interface is determined by the condition that the total atomic flux across it turns to zero:

$$J^{eq} = 0. \tag{14}$$

Taking into account Eq. (13), one can find from Eq. (14) a relation between the kinetically equilibrium solute and PD concentrations at the interface:

$$\frac{c_j^{m\,eq}}{c_j^p} = \frac{\beta_{i_j}^p x_j^{p\,eq} + \left(\delta_{v_j}^m \left(1 - x_j^{p\,eq}\right) + \alpha_{R_j}^p x_j^{eq} \right) c_v^{m\,eq}}{\beta_{i_j}^m x_j^{m\,eq} + \left(\delta_{v_j}^p \left(1 - x_j^{m\,eq}\right) + \alpha_{R_j}^m x_j^{eq} \right) c_{v_j}^{p\,eq}}. \tag{15}$$

In the absence of external perturbations, which violate the conservativity of the system (e.g. irradiation), the conditions of kinetic and thermodynamic equilibrium are equivalent and, therefore, the values entering

Eq. (15) can be considered as thermodynamically equilibrium ones. In this paper we consider thermodynamically nonequilibrium situation caused by cascade-producing irradiation. Nevertheless, the state of kinetic equilibrium (14) in this case is still possible. Therefore, all the values entering Eq. (15) are generally considered as kinetically rather than thermodynamically equilibrium ones.

1.2. DIFFUSION OF SOLUTE IN THE MATRIX

The steady-state solute concentration profile in the matrix is subject to the next diffusion equation:

$$\operatorname{div} J_j^m = 0, \quad J_j^m = -D_j^m \nabla c_j^m, \tag{16}$$

where D_j^m is a solute diffusion coefficient in the matrix.

The normal component of the solute flux across the interface is given by Eq. (9). In the first order in a deviation of the solute concentration at the interface from its kinetic equilibrium value (15), for a spherical particle of radius r_p, Eq. (9) becomes

$$J_j^m(r_p) = \frac{D_j^m}{l}\left[c_j^{m\,eq}(r_p) - c_j^m(r_p)\right], \tag{17}$$

where

$$l = \frac{D_j^m}{\omega_0\left[\beta_{i_j}^m x_j^{m\,eq} + \left(\delta_{v_j}^p\left(1 - x_j^{m\,eq}\right) + \alpha_{R_j}^m x_j^{m\,eq}\right)c_{v_j}^{p\,eq}\right]} \tag{18}$$

is a characteristic length in the model.

One can consider the second boundary condition as follows:

$$c_j^m(\infty) = \overline{c}_j^m, \tag{19}$$

where $\overline{c}_j^m$ is an average solute concentration in the matrix.

The diffusion equation (16) with the boundary conditions, given by Eqs. (17), (19), has the next solution:

$$c_j^m(r) = \overline{c}_j^m + \frac{c_j^{m\,eq}(r_p) - \overline{c}_j^m}{r_p + l}\frac{r_p^2}{r}. \tag{20}$$

With the above results in mind, one can derive the particle velocity in the dimension space as follows:

$$\frac{dr_p}{dt} = -\omega_0 J(r_p) = -\frac{D_j^m}{r_p + l}\frac{c_j^{m\,eq}(r_p) - \overline{c}_j^m}{c_j^p}. \tag{21}$$

From Eq. (20) one can see that

$$\lim_{l/r_p \to 0} c_j^m(r_p) = c_j^{m\,eq}(r_p) \tag{22}$$

and this expression can be used instead of Eq. (17) as the first boundary condition for the diffusion equation (16). This means that, for big particles $(r_p \gg l)$, the model considered here asymptotically gives the same result as the diffusion problem with a given (kinetically equilibrium) solute concentration at the interface, given by the Gibbs-Thomson relation (see e.g. [8]):

$$c_j^{m\,eq}(r_p) = c_j^{m\,eq}\exp(a/r_p), \tag{23}$$

where $c_j^{m\,eq}$ is a kinetically equilibrium solubility limit of solute in the matrix,

$$a = 2\gamma\omega_0/k_B T \tag{24}$$

and γ is a specific nanoparticle-matrix interface energy.

2. SIZE DISTRIBUTION OF NANOPARTICLES

In the absence of irradiation the temporal evolution of the size distribution function of nanoparticles is subject to the Becker-Döring equation [9].

High-energy heavy particles with energies of about several megaelektronvolt in a solid create primary recoil atoms with energies of up to tens kiloelektronvolt which, in their turn, initiate atomic displacement cascades (see e.g. [10]). After the cascade relaxation, some of the involved atoms appear at different from the initial ones spatial positions. This effect is known as cascade mixing (see e.g. [2]). As a result, a minor fraction of atoms is displaced on distances exceeding the period of crystalline lattice. The effect of atomic collision cascades on heterophase nanoparticles was recently studied for the case of copper clusters in iron by the means of molecular dynamics method [11]. The results obtained demonstrate that, if the primary recoil atom is within or on the surface of the nanoparticle, a certain average number of atoms leave the nanoparticle and move to the matrix. This process is called cascade dissolution.

In this way, the kinetic equation for the nanoparticle distribution function $g(n)$ with respect to the number of atoms n, taking into account the effect of irradiation that creates atomic displacement cascades with a volume rate K_c, is the Becker-Döring equation with an additional cascade term in its right-hand side:

$$\frac{dg(n)}{dt} = W_e(n+1)g(n+1) + W_a(n-1)g(n-1) - g(n)\left[W_e(n) + W_a(n)\right] + K_c\omega_0\left[\sum_{k=1}^{k_{\max}} P_c(k, n+k)(n+k)g(n+k) - ng(n)\right], \tag{25}$$

where $W_e(n)$ and $W_a(n)$ are the rates of emission and adsorption of atoms at the nanoparticle interface respectively, and $P_c(k, n+k)$ is a probability that the atomic collision cascade kicks k atoms out of the nanoparticle consisting of initially $(n+k)$ atoms. This probability is subject to the next normalization condition:

$$\sum_{k=1}^{k_{\max}} P_c(k, n+k) = 1. \tag{26}$$

Assuming that $n \gg k_{\max} \geq 1$, in Eq. (25) one can change from the discrete variable n to the continuous one z and expand its right-hand side into the Taylor series up to the second order to obtain the second order differential equation:

$$\frac{\partial g}{\partial t} = \frac{\partial}{\partial z}\left[g\cdot(W_e - W_a) + \frac{1}{2}\frac{\partial}{\partial z}g\cdot(W_e + W_a)\right] + K_c\omega_0\left[\overline{k(z)}g + z\overline{k(z)}\frac{\partial g}{\partial z} + \frac{1}{2}z\overline{k^2(z)}\frac{\partial^2 g}{\partial z^2}\right], \tag{27}$$

where $\overline{k(z)} = \sum_{k=1}^{k_{max}} k\cdot P_c(k, z+k)$ and $\overline{k^2(z)} = \sum_{k=1}^{k_{max}} k^2\cdot P_c(k, z+k)$.

Taking into account that $J_j^m(r_p) = (W_e - W_a)/(4\pi r_p^2)$, from Eqs. (12) and (17), one can derive (see also [5, 6]):

$$W_e = 4\pi r_p^2 D_j^m c_j^{meq}(r_p)/lc_j^p , \tag{28}$$

$$W_a = 4\pi r_p^2 D_j^m c_j^m(r_p)/lc_j^p . \tag{29}$$

Variable z is related to the nanoparticle radius r_p as follows:

$$z = 4\pi r_p^3/3\omega_0 , \tag{30}$$

which allows to change in Eq. (27) to the size distribution function $f(r_p)$:

$$\frac{\partial f}{\partial t} = -\frac{\partial}{\partial r_p}\left[f\cdot\frac{dr_p}{dt} - \frac{\omega_0}{8\pi r_p^2}\frac{\partial}{\partial r_p}f\cdot B(r_p)\right] + K_c\omega_0\left[\frac{\overline{k}}{3} + \frac{5\omega_0\overline{k^2}}{12\pi r_p^3} + \left(\frac{\overline{k}}{3}r_p - \frac{\omega_0\overline{k^2}}{4\pi r_p^2}\right)\frac{\partial}{\partial r_p} + \frac{\omega_0\overline{k^2}}{24\pi r_p}\frac{\partial^2}{\partial r_p^2}\right]\cdot f , \tag{31}$$

where $\overline{k} = \overline{k\,(r_p)}$ and $\overline{k^2} = \overline{k^2(r_p)}$ is assumed for simplicity.

Using Eq. (23) one can express the velocity and the diffusion coefficient in the dimension space in Eq. (31) as follows:

$$\frac{dr_p}{dt} = \frac{D_j^m c_j^{meq}}{c_j^p}\cdot\frac{\exp(a/r_p^c) - \exp(a/r_p)}{r_p + l} , \tag{32}$$

$$B(r_p) = \frac{2D_j^m c_j^{meq}}{c_j^p}\cdot\frac{\exp(a/r_p)}{l} + \frac{dr_p}{dt} , \tag{33}$$

where the critical radius (which turns the rhs of Eq. (32) to zero) is

$$r_p^c = a\Big/\ln\left(\overline{c}_j^m\Big/c_j^{meq}\right). \tag{34}$$

Below it is convenient to change to dimensionless variables $\rho = r_p/r_p^c$ and $\tau = t\cdot D_j^m c_j^{meq}\Big/c_j^p(r_p^c)^2$.

For the new distribution function $\phi(\rho, \tau)$ Eq. (31) takes the form

$$\frac{\partial\phi}{\partial\tau} = -\frac{\partial}{\partial\rho}\left[\phi\cdot\dot{\rho}_\tau - \frac{\varepsilon}{6\rho^2}\frac{\partial}{\partial\rho}\phi\cdot B_\tau(\rho)\right] + C\left[\frac{\overline{k}}{3} + \frac{5\varepsilon\overline{k^2}}{9\rho^3} + \left(\frac{\overline{k}}{3}\rho - \frac{\varepsilon\overline{k^2}}{3\rho^2}\right)\frac{\partial}{\partial\rho} + \frac{\varepsilon\overline{k^2}}{18\rho}\frac{\partial^2}{\partial\rho^2}\right]\cdot\phi , \tag{35}$$

where

$$\dot{\rho}_\tau = [\exp(\alpha) - \exp(\alpha/\rho)]/[\rho + \lambda], \tag{36}$$

$$B_\tau(\rho) = 2\exp(\alpha/\rho)/\lambda + \dot{\rho}_\tau , \tag{37}$$

$$C = \left[c_j^p(r_p^c)^2 K_c\omega_0\right]\Big/\left[D_j^m c_j^{meq}\right], \tag{38}$$

$\lambda = l/r_p^c$, $\alpha = a/r_p^c$, and the inverse number of atoms in a critical cluster is

$$\varepsilon = [3\omega_0]\Big/\left[4\pi(r_p^c)^3\right]. \tag{39}$$

We aim to find a solution of the stationary $(\partial\phi/\partial\tau = 0)$ variant of Eq. (35):

$$\varepsilon\phi'' + p(\rho)\phi' + q(\rho)\phi = 0 , \tag{40}$$

where

$$p(\rho) = \left\{\frac{C\overline{k}}{3}\rho - \dot{\rho}_\tau + \varepsilon\left[\frac{1}{3\rho}\left(\frac{B_\tau}{\rho}\right)' - \frac{C\overline{k^2}}{3\rho^2}\right]\right\}\Bigg/\left(\frac{B_\tau}{6\rho^2} + \frac{C\overline{k^2}}{18\rho}\right), \tag{41}$$

$$q(\rho) = \left\{\frac{C\overline{k}}{3} - (\dot{\rho}_\tau)' + \varepsilon\left[\frac{1}{6}\left(\frac{B_\tau'}{\rho^2}\right)' + \frac{5C\overline{k^2}}{9\rho^3}\right]\right\}\Bigg/\left(\frac{B_\tau}{6\rho^2} + \frac{C\overline{k^2}}{18\rho}\right), \tag{42}$$

and the prime sign means the derivative over ρ.

Provided that $\varepsilon \ll 1$, in the WKB approximation (see e.g. [12]), the asymptotic form of the physically relevant fundamental solution of Eq. (40) is

$$\phi(\rho) = \phi_0 \exp\left\{-\frac{2}{\varepsilon}\int\frac{C\overline{k}\rho^3 - 3\rho^2\dot{\rho}_\tau}{B_\tau + C\overline{k^2}\rho/3}d\rho + 2\int\frac{C\overline{k^2}}{B_\tau + C\overline{k^2}\rho/3}d\rho\right\}\left/\left(B_\tau + \frac{C\overline{k^2}\rho}{3}\right)\right., \tag{43}$$

where ϕ_0 is a normalization coefficient.

For further applications it is convenient to change back to the absolute size distribution function. Then Eq. (43) takes the form

$$f(r_p) = f_0 \exp\left\{-\frac{8\pi}{3\omega_0}\int^{r_p}\frac{\overline{k}\sigma r^3 - 3r^2 v(r)}{u(r) + \overline{k^2}\sigma r/3}dr + 2\int^{r_p}\frac{\overline{k^2}\sigma}{u(r) + \overline{k^2}\sigma r/3}dr\right\}\left/\left(u(r_p) + \overline{k^2}\sigma r_p/3\right)\right., \tag{44}$$

where f_0 is a normalization coefficient,

$$v(r_p) = \frac{\exp(a/r_p^c) - \exp(a/r_p)}{r_p + l}, \tag{45}$$

$$u(r_p) = 2\exp(a/r_p)/l + v(r_p), \tag{46}$$

$$\sigma = \left[c_j^p K_c \omega_0\right]\left/\left[D_j^m c_j^{meq}\right]\right.. \tag{47}$$

When irradiation is absent $(\sigma = 0)$ and the solute concentration is undersaturated $\left(\overline{c}_j^m \le c_j^{meq}\right)$, Eq. (44) reduces to the equilibrium distribution function of sub-critical nanoparticles (heterophase fluctuations) (see also [5, 6]).

3. DISCUSSION AND FITTING OF THE MODEL RESULTS TO SOME EXPERIMENTAL DATA

In this Section we illustrate the model results by fitting them to some experimental data of the atom-probe tomography for the ODS steel 14YWT irradiated with 5 MeV Ni ions at different temperatures [13, 14].

Analysis of these experimental data demonstrates that, under intensive cascade-producing irradiation with 5 MeV Ni ions, the oxide nanoparticles in the 14YWT ODS steel are characterized by the stationary size distribution. Therefore, in this case one can use the stationary distribution function (44) derived in Section 3 for fitting. For this purpose it is necessary to estimate numerically the distribution parameter σ (47).

Consider the grows rate of the average nanoparticle size $\overline{r}_p$ at the coarsening stage, given by the Lifshits-Slyozov formula [3]:

$$\overline{r}_p^3(t) - \overline{r}_p^3(t_0) = \frac{4}{9}\frac{D_j^m c_j^{meq}}{\omega_0 c_j^p}a\omega_0(t - t_0). \tag{48}$$

Eq. (48) can be transformed as follows:

$$\left.\frac{d\overline{n}}{dt}\right|_{dif} = \frac{16\pi}{27}\frac{D_j^m c_j^{meq}}{\omega_0 c_j^p}a, \tag{49}$$

where $\overline{n}$ is an average number of atoms in the nanoparticle. Eq. (49) may be considered as an average growth rate due to diffusion process. From the other hand, atomic collision cascades kick atoms from the nanoparticle with an average rate

$$\left.\frac{d\overline{n}}{dt}\right|_{cas} = -K_c\omega_0\overline{k}\overline{n}. \tag{50}$$

Since, as it was mentioned before, the experimentally obtained distribution function under irradiation demonstrates stationary behavior, the average number of atoms in the nanoparticle must conserve. Therefore, the sum of rhs of Eqs. (49) and (50) is zero and from (47) one finds

$$\sigma = \frac{16}{27}\frac{\pi a}{\omega_0 \overline{k}\overline{n}} = \frac{4a}{9\overline{k}\overline{r}_p^3}. \tag{51}$$

In Figure, a–f we plot the function (44) at finite and zero values of the parameter σ together with the experimental data [13], obtained by the atom-probe tomography, on the size distribution of oxide nanoparticles in 14YWT ODS steel irradiated with 5 MeV Ni ions to 100 dpa at different temperatures.

The next values of the material parameters are used in calculations. We take $\gamma = 1.2\,\mathrm{J/m^2}$ for the specific nanoparticle-matrix interface energy. The mass density of $Y_2Ti_2O_7$ nanoparticles is $\rho = 4.8\cdot10^3\,\mathrm{kg/m^3}$ according to [15]. Therefore, the mean atomic volume in this oxide is $\omega_0 = 0.012\,\mathrm{nm^3}$, almost equal to that of bcc iron. This fact explains the high coherency of the nanoparticle-matrix interface. The average number of atoms, ejected from the nanoparticle by the atomic collision cascade, and its average square are taken $\overline{k} = 3$ and $\overline{k^2} = 9$ respectively, according to results of molecular dynamics simulations [11]. The values of parameters l and σ at different temperatures are given in Table. To find the limit of applicability of the discrete-continuous transformation, one should consider that the radius of the sphere of the unit atomic volume ω_0 is $r_0 = 0.142\,\mathrm{nm}$. A nanoparticle with $r_p = 0.5\,\mathrm{nm}$ contains about 44 atoms. We take the lower limit radius $r_{p\min} = 0.31\,\mathrm{nm}$, corresponding to $n_{p\min} \approx 10$ atoms in the nanoparticle. The value of the critical radius r_p^c was considered infinitely large, corresponding to undersaturated or saturated solute concentrations.
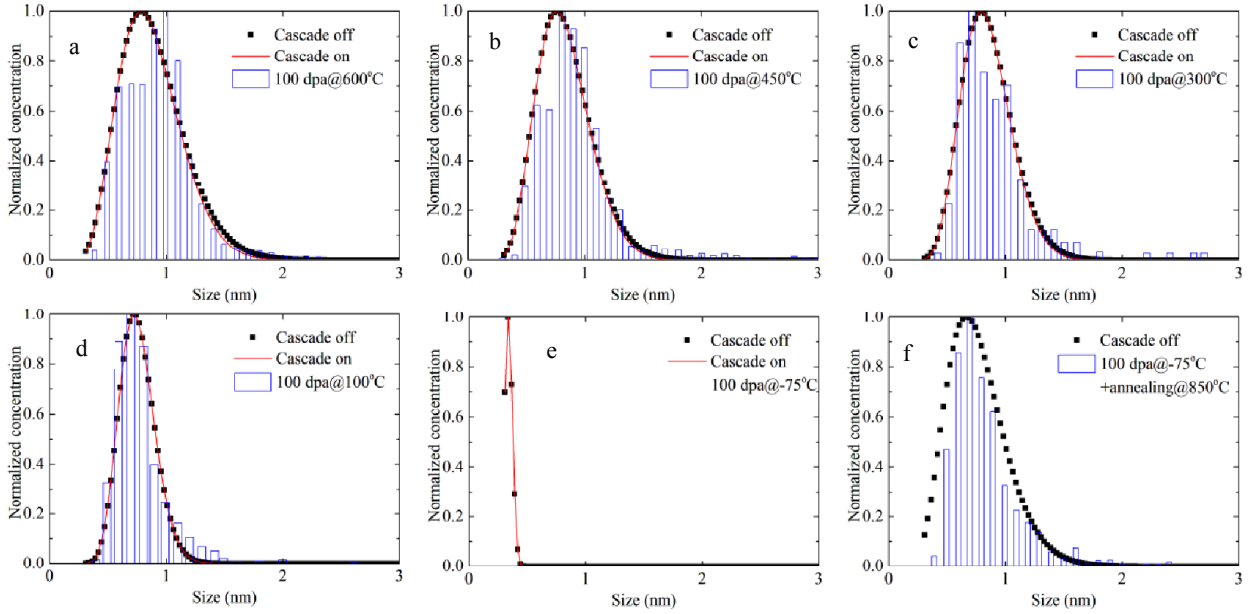
Distribution function parameters

T, °C	600	450	300	100	−75	850 (annealing)
l/r_0	0.035	0.045	0.05	0.1	3	0.045
σ, nm^{-2}	0.354	0.587	1.054	1.619	40.836	0

From Figure, a–c one can see that, at chosen values of the model parameters, the calculated stationary distribution functions with zero (squares) and non zero

(curves) σ are only slightly different in the 1...2 nm range at 600, 450, and 300 °C. In Figure, d the distributions at 100 °C with zero and non zero σ are visually indifferent. In Figure, f bars show the experimental distribution formed after annealing for 5 hours at 850 °C in the preliminary irradiated to 100 dpa at -75 °C sample. In the same Figure, f squares show the plot of stationary distribution without irradiation, in a good agreement with experimental data.

After irradiation to 100 dpa at -75 °C, the atom probe tomography does not detect any oxide nanoparticles. The authors of [13] conclude that they are completely dissolved under irradiation. In Figure, e the distributions calculated with zero and non zero σ demonstrate that at these conditions the oxide nanoparticles become very small, with average size $\bar{r}_p = 0.334\,\text{nm}$, corresponding to the average number $\bar{n}_p \approx 13$ atoms in the nanoparticle. This value is very close to the minimal number of solute atoms in a cluster $n_{\min} \approx 10$, used as a parameter in the cluster search algorithm employed [13]. In this way, the negative experimental result at these conditions can be explained.

Normalized to its maximum size distribution function of oxide nanoparticles at temperatures:
a − 600 °C; b − 450 °C; c − 300 °C; d − 100 °C; e − -75 °C; f − 850 °C. Bars correspond to atom probe tomography data on 5 MeV Ni ion irradiated to 100 dpa ODS steel 14YWT [13]. Squares and curves are given by Eq. (44) with zero and non zero values of the cascade parameter σ respectively.
The values of the model parameters are given in Table and in the main text

As it was mentioned before, at chosen values of the model parameters, the cascade term has only a small numerical effect on the calculated distribution function. Nevertheless, it does not mean that irradiation does not affect the distribution function at all. As follows from Eq. (18), irradiation, which produces nonequilibrium point defects and changes the solute diffusion coefficient in the matrix, affects the value of the distribution parameter *l*. Really, from Table one can see that the value $l = 0.045 \cdot r_0$ is found both at 850 °C without irradiation and at 450 °C under irradiation (see also Figure, b and f). Therefore, it is tempting to assume that changes in the nanoparticle distribution observed after irradiation result from the effect of nonequilibrium point defects rather than from cascade mixing. This assumption is supported by the previous experimental [16] and theoretical [4] findings. This assumption could be checked by performing cascadeless (electron) irradiation experiments at the same temperatures and dose rates.

CONCLUSIONS

Using the previously proposed model of point defect transport in a heterophase medium [4–6], we obtain expressions for absorption and emission rates of solute atoms at the coherent interface as functions of steady state concentrations of nonequilibrium point defects at the opposite interface sides, providing the possibility to study the kinetics of diffusion transformations in solids under irradiation.

For the size distribution function of heterophase nanoparticles under irradiation we obtain a kinetic equation with the cascade term and find its stationary solution in analytical form.

With the proper choice of the parameter values, the model allows a good fit to experimental data [13] on the size distribution function of oxide nanoparticles after 5 MeV Ni ion irradiation to 100 dpa at 600, 450, 300, and 100 °C and after post-irradiation annealing at 850 °C.

We conclude that irradiation affects the distribution of fine oxide nanoparticles by creating nonequilibrium point defects rather than by cascade mixing. The experimental check of this assumption is desirable.

REFERENCES

1. Gary S. Was. *Fundamentals of Radiation Materials Science. Metals and Alloys.* Springer-Verlag Berlin-Heidelberg, 2007, 839 p.

2. Todd R. Allen, Roger E. Stoller, Shinsuke Yamanaka (Editors). *Comprehensive Nuclear Materials.* Elsevier Science, 2012, 3560 p.

3. I.M. Lifshitz, V.V. Slyozov. The kinetics of precipitation from supersaturated solid solutions // *Journal of Physics and Chemistry of Solids.* 1961, v. 19, p. 35-50.

4. A. Borisenko. A model of homogeneous semicoherent interphase boundary for heterophase substitution alloys under irradiation // *Journal of Nuclear Materials.* 2011, v. 410, p. 69-75.

5. O. Borysenko. A new kinetic model for precipitation from solid solutions // *Condensed Matter Physics.* 2015, v. 18, N 2, p. 23603: 1-8.

6. Alexander Borisenko. Classical nucleation theory for solute precipitation amended with diffusion and reaction processes near the interface // *Phys. Rev. E.* 2016, v. 93, p. 052807: 1-7.

7. Alexander Borisenko. Nominal vs. actual supersaturation of solutions // *Journal of Crystal Growth.* 2018, v. 486, p. 122–125.

8. D. Kashchiev. *Nucleation: Basic Theory with Applications.* Butterworth Heinemann, Oxford, 2000, 530 p.

9. R. Becker and W. Döring. Kinetische Behandlung der Keimbildung in übersättigten Dämpfen // *Ann. Phys. (Leipzig).* 1935, v. 416, p. 719-752.

10. J.F. Ziegler, J.P. Biersack, and M.D. Ziegler. *SRIM – the Stopping and Range of Ions in Matter.* SRIM Co., Chester, 2008, 398 p.

11. A. Certain, Voigt H.-J. Lee, T.R. Allen, B.D. Wirth. Investigation of cascade-induced re-solution from nanometer sized coherent precipitates in dilute Fe–Cu alloys // *Journal of Nuclear Materials.* 2013, v. 432, p. 281-286.

12. Carl M. Bender, Steven A. Orszag. *Advanced Mathematical Methods for Scientists and Engineers: Asymptotic Methods and Perturbation Theory.* Springer-Verlag New York-Berlin-Heidelberg, 1999, 593 p.

13. A. Certain, S. Kuchibhatla, V. Shutthanandan, D.T. Hoelzer, T.R. Allen. Radiation stability of nanoclusters in nano-structured oxide dispersion strengthened (ODS) steels // *Journal of Nuclear Materials.* 2013, v. 434, p. 311-321.

14. J. He, F. Wan, K. Sridharan, T. R. Allen, A. Certain, V. Shutthanandan, Y.Q. Wu. Stability of nanoclusters in 14YWT oxide dispersion strengthened steel under heavy ion-irradiation by atom probe tomography // *Journal of Nuclear Materials.* 2014, v. 455, p. 41-45.

15. Jia-Yu Ding et al. Effects of additives on dielectric properties of $Y_2Ti_2O_7$ ceramics //*Journal of Inorganic Materials.* 2011, v. 26, p. 327-331.

16. I. Monnet, P. Dubuisson, Y. Serruys, M.O. Ruault, O. Kaïtasov, B. Jouffrey. Microstructural investigation of the stability under irradiation of oxide dispersion strengthened ferritic steels // *Journal of Nuclear Materials.* 2004, v. 335, p. 311-321.

ТЕОРЕТИЧЕСКОЕ ДОКАЗАТЕЛЬСТВО СТАЦИОНАРНОГО РАСПРЕДЕЛЕНИЯ РАЗМЕРОВ ОКСИДНЫХ НАНОЧАСТИЦ В ДИСПЕРСНО-УПРОЧНЕННОЙ СТАЛИ ПОД КАСКАДООБРАЗУЮЩИМ ОБЛУЧЕНИЕМ

А.А. Борисенко

Модель, разработанная в этой статье, описывает транспорт неравновесных (созданных облучением) точечных дефектов через когерентную границу в гетерофазной среде. В рамках этой модели получено кинетическое уравнение для функции распределения сферических наночастиц второй фазы в твердом растворе, которое включает течение и диффузию наночастиц в пространстве размеров, а также их растворение в каскадах атомных соударений. Получена аналитическая форма и исследовано стационарное решение этого уравнения. Полученый результат хорошо согласуется с экспериментальными данными [A. Certain et al. Journal of Nuclear Materials. (2013) 434, 311] относительно распределения Y-Ti-O-наночастиц в дисперсно-упрочненной оксидами ферритной стали 14YWT, облученной ионами никеля до 100 сна при разных температурах. Сделан вывод, что в этом случае облучение влияет на функцию распределения наночастиц благодаря возникновению неравновесных точечных дефектов, а не каскадному перемешиванию.

ТЕОРЕТИЧНИЙ ДОКАЗ СТАЦІОНАРНОГО РОЗПОДІЛУ РОЗМІРІВ ОКСИДНИХ НАНОЧАСТИНОК У ДИСПЕРСІЙНО-ЗМІЦНЕНІЙ СТАЛІ ПІД КАСКАДОУТВОРЮЮЧИМ ОПРОМІНЕННЯМ

О.О. Борисенко

Модель, що розроблена в цій статті, описує транспорт нерівноважних (створених опроміненням) точкових дефектів через когерентну границю в гетерофазному середовищі. У рамках цієї моделі отримано кінетичне рівняння для функції розподілу сферичних наночастинок другої фази в твердому розчині, що включає плин та дифузію наночастинок у просторі розмірів, а також їх розчинення в каскадах атомних зіткнень. Отримано аналітичну форму та досліджено стаціонарний розв'язок цього рівняння. Отриманий результат гарно узгоджується з експериментальними даними [A. Certain et al. Journal of Nuclear Materials. (2013) 434, 311] щодо розподілу Y-Ti-O-наночастинок у дисперсійно-зміцненій оксидами феритній сталі 14YWT, опроміненій іонами нікелю до 100 зна за різних температур. Зроблено висновок, що в цьому випадку опромінення впливає на функцію розподілу наночастинок завдяки виникненню нерівноважних точкових дефектів, а не каскадному перемішуванню.